Design of Reactive Distillations for Acetic Acid Esterification

Yeong-Tarng Tang, Yi-Wei Chen, Hsiao-Ping Huang, and Cheng-Ching Yu
Dept. of Chemical Engineering, National Taiwan University,
Taipei 106-17, Taiwan

Shih-Bo Hung and Ming-Jer Lee
Dept. of Chemical Engineering, National Taiwan University of Sci. Tech., Taipei 106-07, Taiwan

DOI 10.1002/aic.10519
Published online April 21, 2005 in Wiley InterScience (www.interscience.wiley.com).

The reactive distillation provides an attractive alternative for reaction/separation processes with reversible reactions, especially for etherification and esterification. The discrete nature of chemical species and the complexity of phase equilibria seem to cloud the picture in understanding reactive distillation. The esterifications of acetic acid with five different alcohols, ranging from C_1 to C_5, are studied. First, qualitative relationships between macroscopic process flowsheet and microscopic phase equilibria are established, and the process flowsheets are classified into type I, II, and III for these five systems. Next, a systematic design procedure is devised to optimize the design, based on the total annual cost (TAC) and dominant design variables are identified for different flowsheets. Once quantitative design is available, process characteristic are analyzed and potential problems in process operation are identified. Finally, the economic potentials of these three different flowsheets are explored and explanations are given. The results clearly indicate that it is possible to systemize the design of reactive distillation by qualitatively generating flowsheet from phase equilibria and by quantitatively completing the process flow diagram from a sequential design procedure. Moreover, some of the flowsheets presented in this work cannot be found elsewhere in the open literature. © 2005 American Institute of Chemical Engineers *AIChE J,* 51: 1683–1699, 2005
Keywords: esterification, acetate, reactive distillation, process design

Introduction

Reactive distillation provides an attractive alternative for process intensification, especially for reaction/separation systems with reversible reactions. The literature in reactive distillation has grown rapidly in recent years and the books by Doherty and Malone[1] and Sundmacher and Kienle[2] give updated summaries in the field. Taylor and Krishna[3] give an in-depth review on potential advantages and hardware configurations. As pointed out by Doherty and Buzad,[4] the concept of combining reaction and separation has long been recognized, but rarely put into commercial practice, not until the successful application for the production methyl acetate.[5] Despite clear advantages of simultaneous reaction/separation,[6] commercializing of reactive distillation processes is still quite limited for several reasons. An obvious one is mentioned in[4] "There is almost always a conventional alternative to reactive distillation which is seductive because we have always done it this way". The scenario remains more than a decade later. After the management and technical levels were convinced by the clear edge of reactive distillation, another reason is that the process flowsheets seem to change from case to case (for example,

Correspondence concerning this article should be addressed to C.- C. Yu at ccyu@ntu.edu.tw.

from methyl acetate, to ethyl acetate, to butyl acetate and so on).[5,7,8,9,10,11] Even for the same chemical production (for example, ethyl acetate, butyl acetate, and so on), the flowsheet configurations also vary[8,9,10,11] as one went through the literature. Unlike the conventional distillation, the seemingly case-based design approach and a great deal of process configurations (to choose from) add additional complexity to reactive distillation.

A number of chemical systems have been studied in the literature using reactive distillation columns and among the 74 applications listed in Sundmacher and Kienle,[2] most common applications of reactive distillation are etherification and esterification reactions. The esterification reactions are studied in this work. Esters are of great importance to chemical process industries, and esters are typically produced from the reactions of acid and alcohols under acidic condition. In order to provide possible generalization to the design procedure, in this work, we explore the esterifications of acetic acid with different alcohols ranging from C_1 to C_5. These cover the production of a range of important solvents, methyl acetate, ethyl acetate, iso-propyl acetate, butyl acetate, and amyl acetate, with normal boiling point ranges from 57 to 147°C. In addition to its industrial importance, these five quaternary systems also show complex phase behavior with the number of azeotropes (binary and ternary) varying from 2 to 6 with possible liquid phase splitting.

The objective of this work is intended to provide possible generalization for the design of reactive distillation for esterification reactions with acetic acid. First, the thermodynamic properties for these five quaternary systems are investigated. Next, qualitatively, possible process flowsheets are generated based on the VLLE behaviors of these five systems. Then, design procedures are proposed for different process configuration to determine, quantitatively, the tray numbers in each section of reactive distillation systems and design is optimized based on the total annual cost (TAC). Finally, process characteristics of these five optimally designed reactive distillations are studied, followed by the conclusion.

Reaction Kinetics and Phase Equilibria

Reaction kinetics

The esterification of the acetic acid with different alcohols can be expressed in the following general form

$$\text{acid} + \text{alcohol} \underset{k_{-1}}{\overset{k_1}{\Leftrightarrow}} \text{acetate} + \text{water} \qquad (1)$$

The alcohols studied in this work include methanol (MeOH), ethanol (EtOH), iso-propanol (IPOH), n-butanol (BuOH), and n-pentanol (amyl alcohol, AmOH) and corresponding products are methyl acetate (MeAc), ethyl acetate (EtAc), isopropyl acetate (IPAc), n-butyl acetate (BuAc), and amyl acetate (AmAc), respectively. In this work, we are interested in the solid-catalyzed reaction kinetics for an obvious reason that one can place the reactive zone in different sections of the reactive distillation columns. It is clear that this provides flexibility in process design as opposed to using homogeneous catalysis (for example, sulfuric acid). The solid catalysts used are acidic ion-exchange resin, such as Amberlyst 15 (Rohm and Hass) and Purolite CT179 (Purolite). The solid catalyst can be either immobilized via structured packings such as Katapak-S (Sulzer Chemtech[3,12]) or simply placed inside the tray with certain type of replacement mechanism (Davy Process Technology).

We have not seen too many kinetics data on solid-catalyzed esterification reactions until recently. Literature surveys indicate that most of these data have become available in the past five years[13,14,15,16,17] and Table 1 lists the reaction kinetics used in this study. The reaction rates are expresses in the pseudo-homogeneous model or Langmuir-Hinshelwood and, generally, with the component represented in terms of activity. Moreover, they are all catalyst-weight (m_{cat}) based kinetics. Despite the fact that the kinetic experiments were performed by different groups with somewhat different type of catalysis, we observe certain degree of consistency in the kinetic data (Table 1). The equilibrium constant (K_{eq}, at 363 K) ranges from 1.6 to 16.8, the forward rate constant (k_1, at 363 K) changes from 1.73×10^{-4} to 2.5×10^{-3}, activation energy of the forward reaction varies from 44,000 kJ/kmol to 70,000 kJ/kmol, and the heat of reactions are almost negligible except for the methyl acetate and ethyl acetate systems. Note that for the isopropyl acetate, the $[H^+]$ concentration of 4.6×10^{-3} (mol H^+/kg_{cat}) is assumed to convert the catalyst weight-based expression. Table 1 also shows that the methyl acetate system has the most favorable reaction kinetics catalyst an order of magnitude larger than the rest of the systems.

In applying the reaction kinetics to a reactive distillation, it is assumed that the solid catalyst occupies 50% of the tray holdup volume and a catalyst density of 770 kg/m^3 is used to convert the volume into catalyst-weight (m_{cat}).

Phase Equilibria

To account for nonideal vapor-liquid equilibrium (VLE) and possible vapor-liquid-liquid equilibrium (VLLE) for these quaternary systems, the NRTL[18] model or UNIQUAC model is used for activity coefficients. Table 2 lists the model parameters for these five quaternary systems where EtAc, IPAc and AmAc systems are described by the NRTL model while MeAc and BuAc systems are represented using the UNIQUAC model. Because of the almost atmospheric pressure, the vapor phase nonideality considered is the dimerization of acetic acid as described by the Hayden-O'Conell second virial coefficient model.[19] The Aspen Plus built-in association parameters are used to compute fugacity coefficients.

It should be emphasized the quality of the model parameters (Table 2) is essential to generate correct process flowsheet.[20] Two important steps to validate model parameters are: (1) good prediction of azeotropes, and (2) reasonable description of the liquid-liquid (LL) envelopes for VLLE systems. Correct description of the existence of azeotropes and the ranking of azeotropic temperatures will lead to generating correct residue curve map (RCM), and, consequently, placing separators in the right sections. A reasonable prediction of LL envelope can facilitate possible use of decanter which is often encountered in esterification reactive distillation systems.[10,11,12,20,21] This is also the reason why the NRTL and UNIQUAC models are preferred for activity coefficients. Table 3 reveals that the model parameters give reasonably good description of existing experimental azeotropic data[22] for all 5 systems. Moreover, the models also

Table 1. Kinetic Equations for Five Esterification Systems

System	Kinetic Model (Catalyst)	k_1 (T = 363K)	K_{eq} (T = 363K)
(i)	Pseudo-homogeneous model		
MeAc	(Amberlyst 15)		
	$r = m_{cat}(k_1 a_{HAc} a_{MeOH} - k_{-1} a_{MeAc} a_{H_2O})$	2.49×10^{-3}	16.76
	$k_1 = 2.961 \times 10^4 \exp\left(\frac{-49190}{RT}\right)$	[kmol/(kg_{cat}*s)]	
	$k_{-1} = 1.348 \times 10^6 \exp\left(\frac{-69230}{RT}\right)$		
(ii)	Pseudo-homogeneous model		
EtAc	(Purolite CT179)		
	$r = m_{cat}(k_1 x_{HAc}^{1.5} x_{EtOH} - k_{-1} x_{EtAc} x_{H_2O})$	4.78×10^{-4}	3.50
	$k_1 = 4.24 \times 10^3 \exp\left(\frac{-48300}{RT}\right)$	[kmol/(kg_{cat}*s)]	
	$k_{-1} = 4.55 \times 10^5 \exp\left(\frac{-66200}{RT}\right)$		
(iii)	Langmuir-Hinshelwood/Hougen-Watson model		
IPAc	(Amberlyst 15)		
	$r = m_{cat} \frac{k_1(a_{HAc} a_{IPOH} - a_{IPAc} a_{H_2O}/K_{eq})}{(1 + K_{HAc} a_{HAc} + K_{IPOH} a_{IPOH} + K_{IPAc} a_{IPAc} + K_{H_2O} a_{H_2O})^2}$	2.26×10^{-4}	8.7
	$k_1 = 7.667 \times 10^{-5} \exp\left(23.81 - \frac{68620.43}{RT}\right)$	[kmol/(kg_{cat}*s)]	
	$K_{eq} = 8.7$, $K_{HAc} = 0.1976$, $K_{IPOH} = 0.2396$, $K_{IPAc} = 0.147$, $K_{H_2O} = 0.5079$		
	Assumption: mol H^+/kg_{cat} = 4.6×10^{-3}		
(iv)	Pseudo-homogeneous model		
BuAc	(Amberlyst 15)		
	$r = m_{cat}(k_1 a_{HAc} a_{BuOH} - k_{-1} a_{BuAc} a_{H_2O})$	2.32×10^{-4}	10.9
	$k_1 = 3.3856 \times 10^6 \exp\left(\frac{-70660}{RT}\right)$	[kmol/(kg_{cat}*s)]	
	$k_{-1} = 1.0135 \times 10^6 \exp\left(\frac{-742417}{RT}\right)$		
(v)	Quasi-homogeneous model		
AmAc	(Amberlyst 15)		
	$r = m_{cat}(k_1 C_{HAc} C_{AmOH} - k_{-1} C_{AmAc} C_{H_2O})$	1.13×10^{-6}	1.6
	$k_1 = 31.1667 \exp\left(\frac{-51740}{RT}\right)$	[m^6/(kmol*kg_{cat}*s)]	
	$k_{-1} = 2.2533 \exp\left(\frac{-45280}{RT}\right)$		

*R = 8.314 [kJ/kmol/K], T [K], r [kmol/s], m_{cat} [kg_{cat}], C_i [kmol/m^3], x_i [mole fraction]. (i) Pöpken et al.[13] (ii) Hangx et al.[14] (iii) Gadewar et al.[15] (iv) Gangadwala et al.[11] (v) Lee et al.[17]

predict ternary azeotropes for 4 quaternary systems except the MeAc system (Table 3).

The phase equilibria results reveal that the MeAc quaternary system has two minimum boiling binary azeotropes as shown in Figure 1A and this is the only system without any ternary azeotrope. For the EtAc and IPAc quaternary systems, the models predict three minimum boiling azeotropes and one minimum boiling ternary azeotrope (Figures 1B and 1C). The BuAc quaternary system has three minimum boiling and one maximum boiling binary azeotropes and two

Table 2. Activity Coefficient Models Parameters for Five Esterification Systems

Comp. i / Comp. j	HAc(1) / MeOH(2)	HAc(1) / MeAc(3)	HAc(1) / H_2O(4)	EtOH(2) / MeAc(3)	MeOH(2) / H_2O(4)	MeAc(3) / H_2O(4)
			(i) MeAc system—UNIQUAC (Pöpken et al.[13])			
a_{ij}	−0.97039	0.43637	0.051007	0.71011	−3.1453	−0.010143
a_{ji}	2.0346	−1.1162	0.29355	−0.72476	2.0585	−0.96295
b_{ij} (K)	−390.26	62.186	−422.38	−62.972	575.68	−593.7
b_{ji} (K)	−65.245	−81.848	98.12	−326.2	−219.04	265.83
$c_{ij\,j}$ (K^{-1})	0.0030613	−0.00027235	0.00024019	−0.001167	0.0060713	0.0021609
$c_{ji\,j}$ (K^{-1})	−0.003157	0.0013309	0.000076741	0.0023547	−0.0070149	−0.00020133
			(ii) EtAc System—NRTL (Tang et al.[26])			
Comp. i / Comp. j	HAc(1) / EtOH(2)	HAc(1) / EtAc(3)	HAc(1) / H_2O(4)	EtOH(2) / EtAc(3)	EtOH(2) / H_2O(4)	EtAc(3) / H_2O(4)
a_{ij}	0	0	−1.9763	1.817306	0.806535	−2.34561
a_{ji}	0	0	3.3293	−4.41293	0.514285	3.853826
b_{ij} (K)	−252.482	−235.279	609.8886	−421.289	−266.533	1290.464
b_{ji} (K)	225.4756	515.8212	−723.888	1614.287	444.8857	−4.42868
c_{ij}	0.3000	0.3000	0.3000	0.1000	0.4000	0.3643
			(ii) IPAc System—NRTL (Gadewar et al.[15])			
Comp. i / Comp. j	HAc(1) / IPOH(2)	HAc(1) / IPAc(3)	HAc(1) / H_2O(4)	IPOH(2) / IPAc(3)	IPOH(2) / H_2O(4)	IPAc(3) / H_2O(4)
b_{ij} (K)	−141.6447911	70.96532461	−110.5806744	191.0869653	20.05742325	415.478762
b_{ji} (K)	40.96255662	77.9005536	424.0603422	157.1039255	833.0422748	1373.462808
c_{ij}	0.3048	0.3014	0.2997	0.3000	0.3255	0.3000
			(iv) BuAc System—UNIQUAC (Venimadhavan et al.[32])			
Comp. i / Comp. j	HAc(1) / BuOH(2)	HAc(1) / BuAc(3)	HAc(1) / H_2O(4)	EtOH(2) / BuAc(3)	BuOH(2) / H_2O(4)	BuAc(3) / H_2O(4)
b_{ij} (K)	66.315	150.193	172.92	−41.53679	−34.227	−345.098
b_{ji} (K)	−74.62672	−358.447	−265.6904	−12.4	−292.4746	−232.247
			(v) AmAc System—NRTL (Chiang et al.[21])			
Comp. i / Comp. j	HAc(1) / AmOH(2)	HAc(1) / AmAc(3)	HAc(1) / H_2O(4)	AmOH(2) / AmAc(3)	AmOH(2) / H_2O(4)	AmAc(3) / H_2O(4)
b_{ij} (K)	−316.8	−37.943	−110.57	−144.8	100.1	254.47
b_{ji} (K)	178.3	214.55	424.018	320.6521	1447.5	2221.5
c_{ij}	0.1695	0.2000	0.2987	0.3009	0.2980	0.2000

[a] *NRTL model*: $$\ln \gamma_i = \frac{\sum_{j=1}^{nc} \tau_{ji} G_{ji} x_j}{\sum_{k=1}^{nc} G_{ki} x_k} + \sum_{j=1}^{nc} \frac{x_j G_{ij}}{\sum_{k=1}^{nc} G_{kj} x_k} \left[\tau_{ij} - \frac{\sum_{k=1}^{nc} x_k \tau_{ki} G_{kj}}{\sum_{k=1}^{nc} G_{kj} x_k} \right].$$

$$G_{ij} = \exp(-\alpha_{ij}\tau_{ij}),\ \tau_{ij} = a_{ij} + \frac{b_{ij}}{T},\ \alpha_{ij} = c_{ij},\ G_{ii} = 1 \text{ and } \tau_{ii} = 0.$$

[b] *UNIQUAC model*: $$\ln \gamma_i = \ln \frac{\Phi_i}{x_i} + \frac{z}{2} q_i \ln \frac{\theta_i}{\Phi_i} + l_i - \frac{\Phi_i}{x_i} \sum_{j=1}^{nc} x_j l_j + q_i' \left[1 - \ln \left(\sum_{j=1}^{nc} \theta_j' \tau_{ji} \right) - \sum_{j=1}^{nc} \frac{\theta_j' \tau_{ij}}{\sum_{k=1}^{nc} \theta_k' \tau_{kj}} \right].$$

$$\Phi_i = \frac{r_i x_i}{\sum_{k=1}^{nc} r_k x_k},\ \theta_i = \frac{q_i x_i}{\sum_{k=1}^{nc} q_k x_k},\ \theta_i' = \frac{q_i' x_i}{\sum_{k=1}^{nc} q_k' x_k}.$$

$$\tau_{ij} = a_{ij} + \frac{b_{ij}}{T} + c_{ij} T, \quad l_i = \frac{z}{2}(r_i - q_i) - (r_i - 1) \text{ and } z = 10.$$

ternary azeotropes (Figure 1D) and the AmAc system gives three minimum boiling binary azeotropes and two ternary azeotropes (Figure 1E). It is important to notice that, for EtAc, IPAc, BuAc, AmAc systems, the minimum temperature inside the composition space is the *ternary minimum boiling azeotrope*. Significant LL envelopes are also observed for these five quaternary systems, especially for the acid free ternary systems (Figure 1). The MeAc, EtAc, & IPAc systems show type I LL envelopes while the BuAc & AmAc systems give type II envelopes as shown in Figure 1. The tie lines slop into pure water node and it becomes more evident as the carbon number in the alcohol increases. That is relatively pure water can be recovered from the LL separation for 4 out of these 5 systems (except the MeAc system) and the separation (for achieving high purity water) becomes easier as the carbon number in the alcohol in-

Table 3. Azeotrope Data for Five Esterification Systems

(i) MeAc	(ii) EtAc	(iii) IPAc	(iv) BuAc	(v) AmAc
MeOH/MeAc	EtOH/EtAc/H_2O	**IPOH/IPAc/H_2O**	**BuOH/BuAc/H_2O**	**AmOH/AmAc/H_2O**
53.65°C	70.09°C	**74.22°C**	**90.68°C**	**94.71°C**
(0.3407, 0.6593)	(0.1069, 0.6073, 0.2858)	**(0.2377, 0.4092, 0.3531)**	**(0.0864, 0.206, 0.7075)**	**(0.0488, 0.1292, 0.822)**
54°C	*70.23°C*	*75.5°C*	*89.4°C*	*94.9°C*
(0.359, 0.641)	*(0.1126, 0.5789, 0.3085)*	*(0.1377, 0.4938, 0.3885)*	*(0.111, 0.135, 0.754)*	*(0.046, 0.107, 0.847)*
MeAc/H_2O	**EtAc/H_2O**	**IPAc/H_2O**	**BuAc/H_2O**	**AmAc/H_2O**
56.43°C	**70.37°C**	**76.57°C**	**90.96°C**	**94.90°C**
(0.8904, 0.1096)	**(0.6869, 0.3131)**	**(0.5981, 0.4019)**	**(0.2823, 0.7177)**	**(0.1696, 0.8304)**
56.4°C	*70.38°C*	*76.6°C*	*90.2°C*	*95.2°C*
(0.8804, 0.1196)	*(0.6885, 0.3115)*	*(0.5982, 0.4018)*	*(0.278, 722)*	*(0.166, 0.834)*
	EtOH/EtAc	IPOH/IPAc	**BuOH/H_2O**	**AmOH/H_2O**
	71.81°C	78.54°C	**92.62°C**	**95.80°C**
	(0.4572, 0.5428)	(0.5984, 0.4016)	**(0.2451, 0.7549)**	**(0.1512, 0.8488)**
	71.81°C	*80.1°C*	*92.7°C*	*95.8°C*
	(0.462, 0.538)	*(0.6508, 3492)*	*(0.248, 0.752)*	*(0.146, 0.854)*
	EtOH/H_2O	IPOH/H_2O	BuOH/BuAc	HAc/AmOH/AmAc
	78.18°C	80.06°C	116.85°C	139.89°C
	(0.9016, 0.0984)	(0.6691, 0.3309)	(0.7847, 0.2153)	(0.2225, 0.6108, 0.1667)
	78.174°C	*82.5°C*	*116.2°C*	
	(0.9037, 0.0963)	*(0.6875, 0.3125)*	*(0.73, 0.27)*	
			HAc/BuOH/BuAc	HAc/AmOH
			121.58°C	140.07°C
			(0.4182, 0.2396, 0.3423)	(0.2585, 0.7415)
			HAc/BuOH	
			123.21°C	
			(0.5359, 0.4641)	

* Heteroazeotropes in boldface.
**Experimental data (Horsly[22]) in italics.

creases. For EtAc system, the ternary minimum boiling azeotrope lies closely on the edge of LL envelope. For IPAc, BuAc, & AmAc systems, the ternary minimum boiling azeotrope lies inside the LL envelope and it moves further inside the LL zone as the carbon number increases. As will be shown later, this has important implications in the flowsheet development.

Process Flowsheets

In this section, attempts are made to generate flowsheet for high purity acetates using the combination of stripper, rectifier, reactive section, and possibly a decanter. That is to device hybrid reactive distillation systems to produce commercial grade acetates.

Type I Flowsheet - MeAc

In reactive distillation, typically, the *heavy* reactant is fed from the *top* of the reactive section and the *light* reactant goes into the *bottom* part of the reactive zone. For methyl acetate system, the heavy reactant is the acid (HAc) and the light reactant is the alcohol (MeOH). If the reactive zone consumes all the acid, we are dealing with the separation of the H_2O/MeOH/MeAc, an almost ternary system, in the stripping section. Figure 3A indicates that most of the composition space lead to a rather pure H_2O in the bottom of the reactive distillation. On the other hands, if we react away most of the alcohol toward the top section of the reactive zone, in the rectifying section, we are separating HAc/MeAc with small amount of H_2O. Again, the RCM in Figure 3A shows that it is possible to obtain relatively high purity MeAc, despite being a saddle in the RCM rotation. This is exactly the methyl acetate process configuration (with a little modification, first proposed by Agreda et al.[5] and studied by many others.[1,7]

This process flowsheet can be understood from the boiling point (including azeotropes) temperatures ranking (Table 4). The heavy product of the reaction, H_2O is withdrawn from the bottoms, and the light product MeAc is taken out from the top. The azeotropes play little role in the separation sections except that the top product is a saddle (ultimately the RCM will end at the MeAc/H_2O azeotrope, 56.43°C). This will cause some problems in control and operation. Nevertheless, at design stage, it is possible to achieve high purity products at both ends with the type I flowsheet (Figure 2A).

Type II Flowsheet - EtAc & IPAc

The boiling point temperature ranking may suggest that we can use the type I flowsheet for the EtAc production with the EtAc and H_2O withdrawn the top and the bottom of the column. Indeed, it was simulated by several researchers,[23,24] but the purity level (~80%) is far from the product specification and further purification is needed. In analogy to the MeAc system, we are looking at the H_2O/EtOH/EtAc ternary system for the stripping section. It becomes obvious that the EtAc system has a much complicated phase behavior and, in particular, three distillation boundaries are found for the H_2O/EtOH/EtAc system (Figure 3B). Moreover, we also have EtOH/H_2O (78.18°C) azeotrope that may prevent obtaining high purity H_2O if one is performing the separation along the EtOH-H_2O edge. Actually, Lee[25] also shows that only one double-feed column (type-I flowsheet) cannot produce pure EtAc and further purification is needed. However, we also observe the

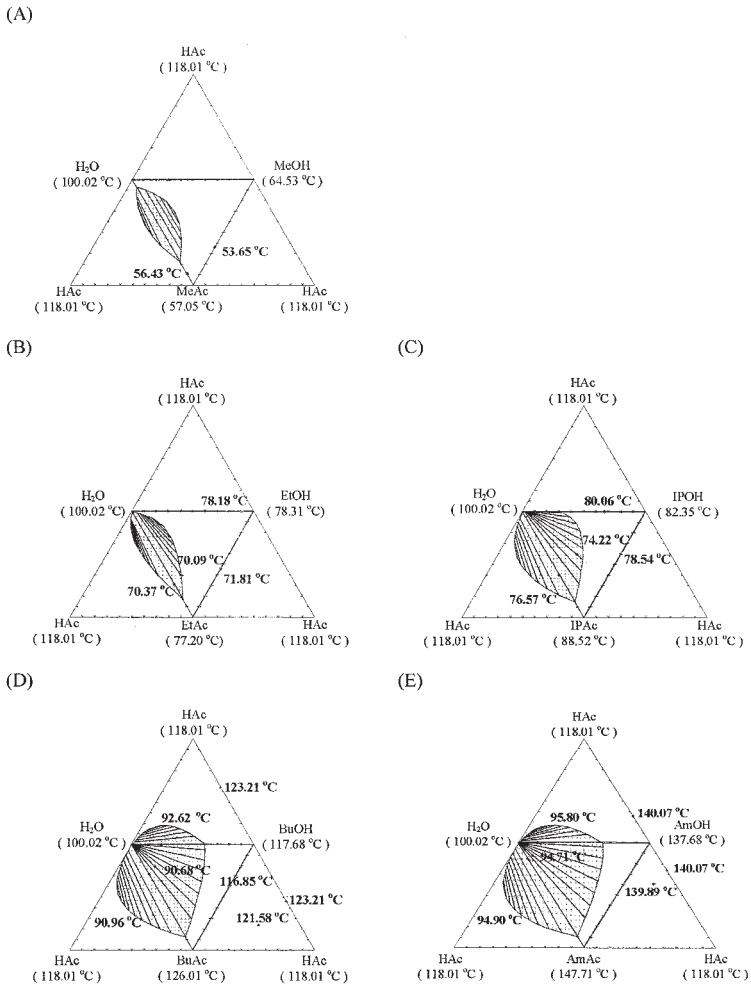

Figure 1. Liquid-liquid envelopes and azettropic temperature and NBP temperatures of pure component.

ternary azeotrope EtOH/EtAc/H_2O has the lowest temperature (70.09°C) (Table 4 and Figure 1B). Furthermore, the azeotrope lies on the edge of the LL envelope with the tie lines slop toward relatively high purity H_2O (Figure 1B). Therefore, when most of the acid is consumed in the reactive section, we end up close to the ternary azeotrope at the top of the column between the EtAc/H_2O (70.37°C) binary azeotrope and the ternary azeotrope, for example, Figure 3B. A decanter is placed to remove the heavy product H_2O from the aqueous with the organic phase further processed to obtain high purity EtAc in a stripper (Figure 3B), with the top recycled back to the decanter. This is the basic process configuration presented by Burkett and Rossiter[8] and Tang et al.[26] which is denoted as type II process hereafter (Figure 2). Note that the products of both the first column (reactive zone + rectifier) and the second column (stripper) are all nodes (stable or unstable) and they possess much better operability as compared to the MeAc system.

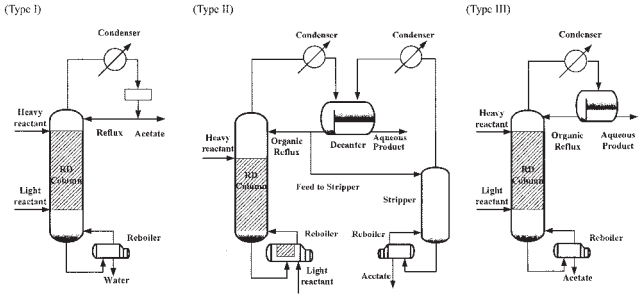

Figure 2. Three possible flowsheets for these five esterification systems systems.

In contrast to MeAc and EtAc synthesis, the information about isopropyl acetate synthesis with acetic acid in a reactive distillation process can hardly be found in the literature except for the VLE and kinetics data.[1,27] The RCM of IPAc system in Figure 3C clearly suggests that the type II process is an ideal candidate for the IPAc synthesis using a reactive distillation. IPAc system is even more favorable with the type II flowsheet than the EtAc system for the reasons that it has a larger LL envelope with a minimum boiling ternary azeotrope (74.22°C) located further inside the LL zone with tie lines mostly point to the high-purity H_2O corner. Once the H_2O is removed from the aqueous phase of the decanter, part of the organic distillate is fed to a stripper by removing high purity IPAc from the bottoms and the top product of the stripper is recycled back to the decanter (Figures 2 and 3C). Also, note that the top products of both the reactive distillation (1st column in Figure 2) and the stripper (2nd column in Figure 2) all point toward the ternary

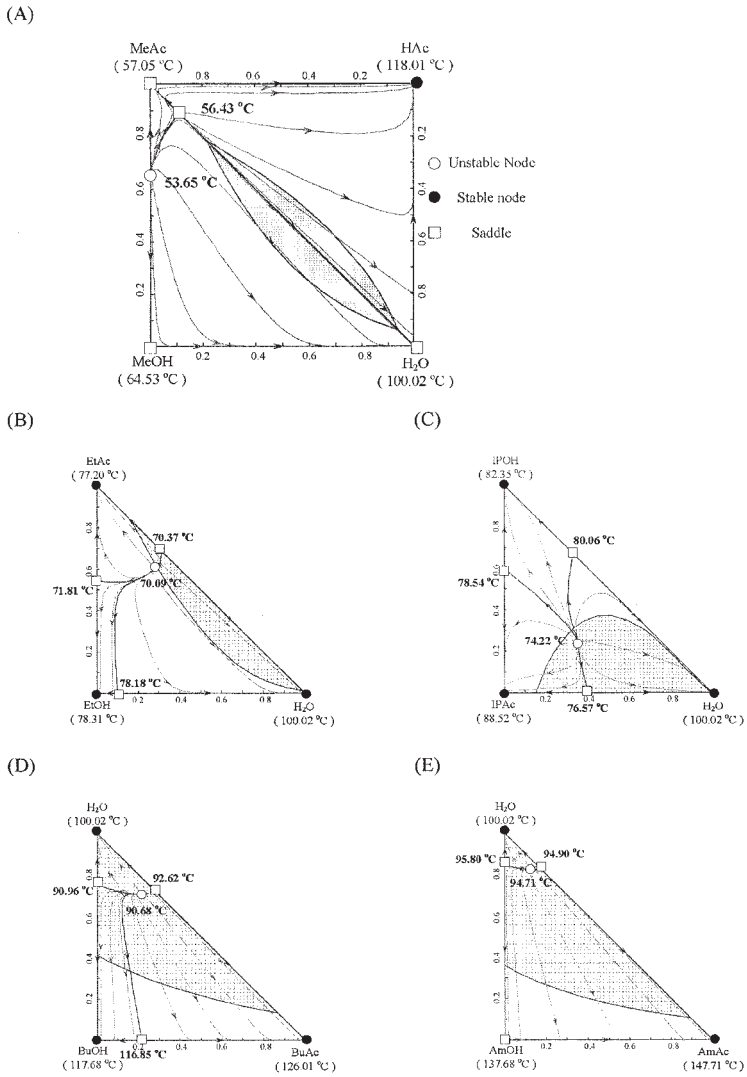

Figure 3. RCM and LL envelope for combinations of ternary systems.

azeotrope (an unstable node) while the bottom product of the stripper slops to a stable node (IPAc corner in Figure 3C).

Type III Flowsheet - BuAc & AmAc

The boiling point temperature rankings in Table 4 reveal that butyl acetate differs from the IPAc in that the acetate is the highest boiling component. That implies that we can remove the acetate from the column base, even from a hybrid reactive distillation. Moreover, the minimum boiling azeotrope between BuOH and H_2O is a heterogeneous one (Figure 1D) and this leads to a type II LL envelope in the BuAc/BuOH/H_2O ternary composition space. Figure 1D also reveals that the two-liquid zone in the ternary system constitutes more than 50% of the composition space. However, the BuAc and IPAc systems also share a common characteristic: a minimum boiling ternary azeotrope exists in the acetate/alcohol/water ternary system and it locates inside the LL envelope as shown in Figure 1D. This immediately suggests a decanter should be placed in the column top by removing almost pure water from the aqueous phase. Unlike the type II flowsheet, the heavy boiling acetate implies that we can totally recycle the organic phase back to the column and withdraw the acetate from the bottoms. The scenario suggests the type III flowsheet for the BuAc as shown in Figure 2. That is quite similar to a typical column with the reactive zone locates in the middle with a decanter to perform LL separation. The removal of water should be relatively easy with the significant LL envelope and the favorable RCM as a result of the ternary azeotrope (Figure 3D). This is exactly the flowsheet proposed by several different research groups.[10,11,16,28]

The amyl acetate system also shows a similar VLLE characteristic with an even larger LL envelope for the acetate/alcohol/water system as shown in Figure 1E. The larger LL zone suggests that the LL separation could be even easier for the AmAc system (as compared to the BuAc system). This naturally leads to the type III flowsheet by removing rather pure water from the top and heavy acetate from the bottoms. It is also observed that amyl alcohol is the second highest boiling pure component, which is different from the BuAc system where the acid is the one.

It is interesting to see the gradual transition in the VLLE

Table 4. Ranking of Azeotropic Temperatures and Pure Component NBP Temperatures

(i) MeAc	(ii) EtAc	(iii) IPAc	(iv) BuAc	(v) AmAc
MeOH/MeAc	EtOH/EtAc/H_2O	**IPOH/IPAc/H_2O**	**BuOH/BuAc/H_2O**	**AmOH/AmAc/H_2O**
53.65°C	70.09°C	**74.22°C**	**90.68°C**	**94.71°C**
MeAc/H_2O	**EtAc/H_2O**	**IPAc/H_2O**	**BuAc/H_2O**	**AmAc/H_2O**
56.43°C	**70.37°C**	**76.57°C**	**90.94°C**	**94.90°C**
MeAc	EtOH/EtAc	IPOH/IPAc	**BuOH/H_2O**	**AmOH/H_2O**
57.05°C	71.81°C	78.54°C	**92.62°C**	**95.80°C**
MeOH	EtAc	IPOH/H_2O	H_2O	H_2O
64.53°C	77.20°C	80.06°C	100.02°C	100.02°C
H_2O	EtOH/H_2O	IPOH	BuOH/BuAc	HAc
100.02°C	78.18°C	82.35°C	116.85°C	118.01°C
HAc	EtOH	IPAc	BuOH	AmOH
118.01°C	78.31°C	88.52°C	117.68°C	137.68°C
	H_2O	H_2O	HAc	HAc/AmOH/AmAc
	100.02°C	100.02°C	118.01°C	139.89°C
	HAc	HAc	HAc/BuOH/BuAc	HAc/AmOH
	118.01°C	118.01°C	121.58°C	140.07°C
			HAc/BuOH	AmAc
			123.21°C	147.71°C
			BuAc	
			126.01°C	

*Heteroazeotropes in boldface.

system (for example, Figures 1 and 3) as the carbon number in the alcohols increases, despite via discrete change between chemical species. It is even more interesting to find out the jumps between process flowsheets (Figure 2) as the VLLE characteristics (for example, ranking of boiling points in Table 4) pass through some critical points. Qualitatively, it seems that we can determine the type of flowsheet by simply examining the VLLE behavior. These observations will be examined carefully in the next section.

Finally, it is also observed that, despite of seemingly different process configurations, these three flowsheets (Figure 2) share a common characteristic. That is they all consist of three major elements: a reactive section, a rectifier, and a stripper with somewhat different arrangement.

Steady State Design

The total annual cost (TAC) of Douglas[29,20,21] is used to evaluate different designs. The TAC is defined as

$$\text{TAC} = \text{operating cost} + \frac{\text{capital cost}}{\text{payback year}} \tag{2}$$

where the operating cost includes the costs of steam, cooling water, and catalyst, and the capital cost covers the cost of the column, trays, heat exchangers. Appendices A and B give the detailed step for computing the TAC. In this work, a payback year of 3 is used and the catalyst life of 3 months is also assumed.

Design procedure

As pointed out earlier, despite having different process configurations, these flowsheets all consist of a rectifier, a stripper, and a reactive section. Obvious design parameters are the number of rectifying tray (N_R), the number of stripping trays (N_S), and the number of reactive trays (N_{rxn}). In addition to the tray numbers, another set of important design parameters are the feed tray locations (NF_{Acid} & $NF_{Alcohol}$).[20,28] In theory the equalmolar feed flow rates ($F_{Acid} = F_{Alcohol}$) should be economically optimal, but for the type II flowsheet, the feed ratio ($FR = F_{Acid}/F_{Alcohol}$) is also an important design variable. Thus, potential design variables for these 3 flowsheets are: N_R, N_S, N_{rxn}, NF_{Acid} & $NF_{Alcohol}$, and FR. Once the column configuration is specified, we are left with two degrees of freedoms for type I & III processes and three degrees of freedoms for type II flowsheet. In a type I process, two product specifications are given to define the simple one-feed-two-product column and typically reflux flow and heat input are used to meet the specification. For the type II process, one product purity, the organic reflux ratio, and no aqueous reflux are used to define the flowsheet. The organic reflux ratio, in a sense, defines the distribution of heat input ($Q_R/Q_{R,\ S}$) between the RD column and the stripper. Typically, this degree of freedom is used to drive the acid purity level to an acceptable level. Note that there is no product withdrawal from the bottoms of the RD column, so the boilup rate is the sum of total feed and reflux flow and no degree of freedom left once the reflux flow is given. The third degree of freedom should be the aqueous reflux ratio. Because the water content in the aqueous phase is primarily determined by the shape of the LL zone, the aqueous reflux ratio has little effect on the product purity and we assume no reflux for the aqueous phase. For the type III flowsheet, one product purity and no aqueous reflux are used to define the flowsheet. That means the top product is withdraw from the aqueous phase and a total reflux for the organic phase. For a type III process, generally we adjust the heat duty to achieve desired product purity.

Once the dominant design variables are identified, a systematic design procedure can be devised for all three flowsheets. All the simulations are carried out using ASPEN PLUS with the RADFRAC module provided with FORTRAN subroutines for the reaction rates. For a system with a given production rate with product specifications, the design steps are

1. Set the reactants feed ratio to 1 initially (that is, $FR = F_{Acid}/F_{Alcohol} = 1$).
2. Fix a number of reactive trays (N_{rxn}).
3. Place the heavy reactant feed (NF_{heavey}) on the top of the

reactive zone and introduce the light reactant feed (NF_{light}) on the lowest tray of the reactive zone.

4. Guess the tray numbers in the rectifying section (N_R) and the stripping section (N_S).

5. Change the reflux flow (R) and heat input (Q_R) (type I flowsheet) or organic reflux flow (R) and stripper heat input (Q_{R_S}) (type II flowsheet) or heat input (Q_R) (type III flowsheet) until the product specification is met.

6. Go back to (4) and change N_R and N_S until the TAC is minimized.

7. Go back to (3) and find the feed locations (NF_{heavey} & NF_{light}) until the TAC is minimized.

8. Go back to (2) and vary N_{rxn} until the TAC is minimized.

9. Go back to (1) and change the feed ratio (FR) until the TAC is minimized (for type II flowsheet only).

It seems strange to devise a sequential design procedure when it may have been done simultaneously. Extensive experience on reactive distillation simulation indicates that the algorithm for the reactive distillation is much less robust as compared to typical distillation. It is more practical to carry out the simulation sequentially. In the work we assume the catalyst occupies 50% of the holdup volume in a reactive tray, the column diameter is sized using the short-cut method of Douglas[29] and a weir height of 10.16 cm (Type I & II) or 5.08 cm (Type III) is assumed for the reactive tray. That is the catalyst weight is fixed once the column diameter is determined.

Optimal Design

Type I - MeAc

For the MeAc system, we assume an equalmolar feed rates ($FR = 1$), thus the dominant variables for optimization become: N_R & N_S, N_{rxn}, and NF_{heavy} & NF_{light}. Top graph of Figure 4 shows that N_R & N_S have little impact on the TAC, despite showing a minimum as N_S varies. Note that this profile is obtained by fixing the feeds to the top and bottom of the reactive section (for example, Figure 2). Flat profiles are also observed as we change the number of reactive trays. The most dominant optimization variables are the *feed tray locations* as shown in Figure 4. The results indicate that the light reactant (MeOH) should be fed to tray 13 (counting the tray number from bottoms up) and the heavy reactant (HAc) should be introduced to tray 36. Note that these two trays lie inside the reactive zone (but not on the top and bottom).

Type II - EtAc & IPAc

The type II flowsheet differs from the type I in that the reactive zone extends to the column base of the first column (called RD column) and, therefore, a much larger holdup is expected in the bottom of the RD column (Figure 2). In this work, the column base holdup is taken to be 10 times of the tray holdup. We also assume the feed ratio of the reactant can be changed and this lead to the following optimization variables: N_R & N_S, N_{rxn}, NF_{heavy} & NF_{light}, and FR. For EtAc, the results (Figure 6) indicate that the *number of trays in the rectifying section* in the RD column (N_R) is one of the dominant optimization variables while the N_S shows little impact on the TAC once N_R is fixed. Relatively, variation of N_{rxn} results in a rather small change in the TAC. Note that the top two graphs in Figure 6 are obtained by fixing the feeds to the top and

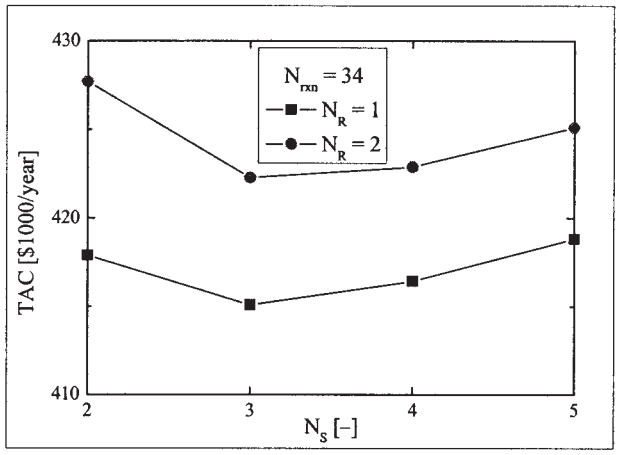

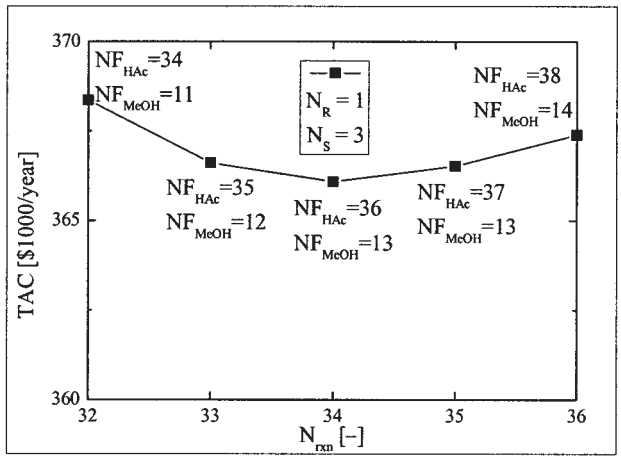

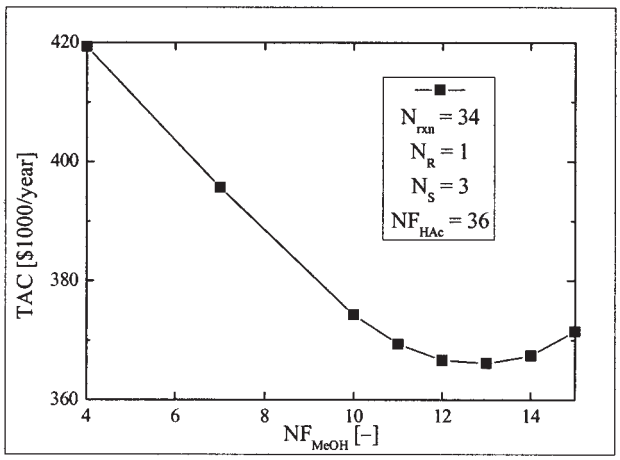

Figure 4. Effects of design variables on TAC for the MeAc system.

bottoms of the reactive section. As for the feed tray locations, the optimal feed tray for the heavy reactant (HAc) is the column base, despite with small difference in the TAC's. This is understandable because we have the largest catalyst holdup in the reboiler and this leads the same feed location for both

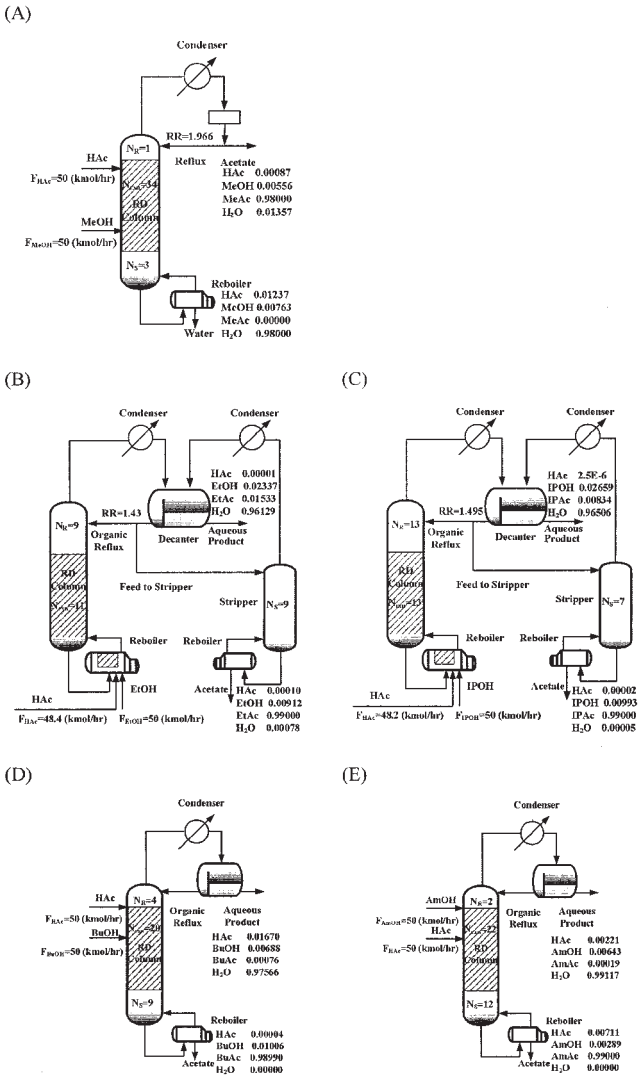

Figure 5. Optimized process flowsheets for these five esterification systems.

reactants. Surprisingly, another dominant variable for optimization is the *feed ratio* (*FR*) and result shows that a little alcohol excess is preferred because this facilitates the top of the RD column falls inside the LL envelope leaving trace amount of acid. The reboiler duty in the RD column reveals this fact as shown in Figure 6. Numerical simulation results indicate that the minimum number of reactive trays needed to achieve the desired purity (mole fraction of acetate equal to 0.99 and acid purity less than 100 ppm) is 7 (that is, $N_{rxn,min} = 7$). Also note that, for the same specification, the operating window for the feed ratio ranges from 0.962 to 0.98 and this implies some feedback control is necessary to maintain the feed ratio.

For the IPAc system, we have the same optimization variables for the type II flowsheet. Again, the results (Figure 7) reveal that N_S has little impact on the TAC and, as expected, both reactant feeds should be introduces to the reboiler. Again, the *number of trays in the rectifying section* (N_R) is one dominant variable for optimization. Relatively, changes in N_{rxn} result in a rather small variation in the TAC. Note that the top two graphs in Figure 7 are obtained by fixing the feeds to the

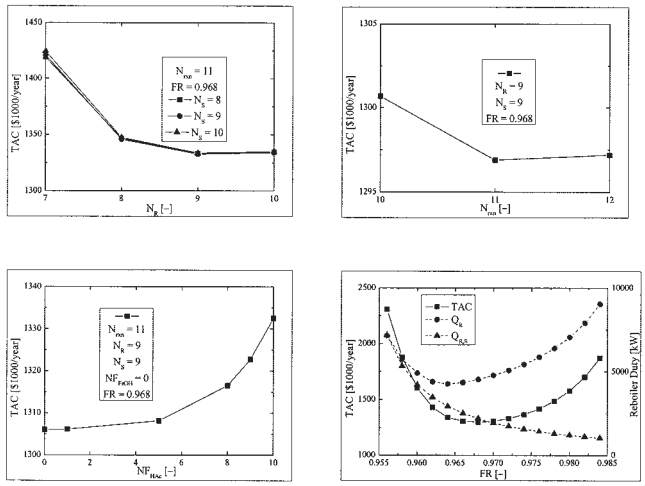

Figure 6. Effects of design variables on TAC for the EtAc system.

top and bottoms of the reactive section. The other is the *feed ratio* (*FR*) as shown in Figure 7. The results also indicate a little alcohol excess is favorable to obtain as easier LL separation. For the IPAc process, the minimum number of reactive trays needed to achieve the desired purity (mole fraction of acetate equal to 0.99 and acid purity less than 100 ppm) is 9 (that is, $N_{rxn,min} = 9$). The operating window for the feed ratio ranges from 0.946 to 0.99 for the desired specification. Again, some feedback mechanism is needed to adjust the feed ratio.

Type III - BuAc & AmAc

The type III flowsheet has been studied by several researchers.[20,21] In theory, we have the following optimization variables: N_R & N_S, N_{rxn}, and NF_{heavy} & NF_{light}. For the BuAc system, the top graph of Figure 8 shows that variations in N_R and N_S result in a rather small change in the TAC. Note that the TAC's are obtained by fixing the feeds to the top and bottoms of the reactive section. The bottom graph in Figure 8 clearly shows that the *feed locations* are the most important optimiza-

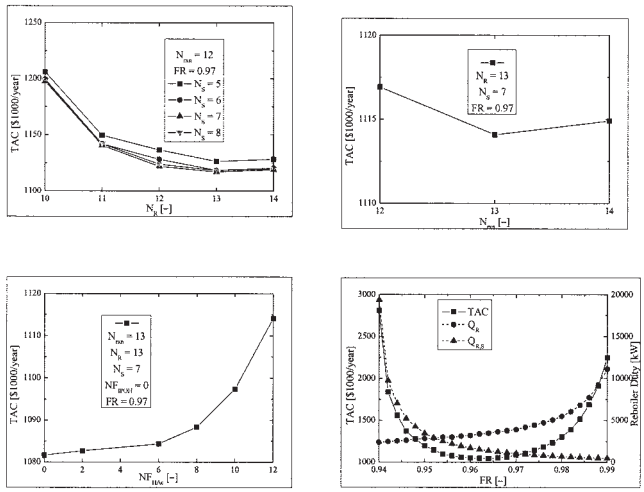

Figure 7. Effects of design variables on TAC for IPAc system.

tion variables as shown in Figure 8 where significant TAC is saved by simply varying the feed locations. This can be understood because we need to arrange the feeds such that optimal reactant and temperature profiles can be achieved in the reactive section.

For the AmAc system, top graph of Figure 9 shows that variations in N_R and N_S result in a rather small change in the TAC. Again, the TAC's are obtained by fixing the feeds to the top and bottoms of the reactive section. The bottom graph in Figure 9 clearly indicates that, again, the feed locations are the dominant optimization variables as compared to other variables, such as N_R & N_S and N_{rxn}.

The optimization results show an interesting fact that different flowsheets give rise to different dominant optimization variables. They are: (1) NF_{heavy} & NF_{light} for the type I flowsheet, (2) N_R and FR for the type II flowsheet, and (3) NF_{heavy} & NF_{light} for the type III flowsheet. Table 5 summarizes the optimal designs for these five systems and the flowsheets are given in Figure 5.

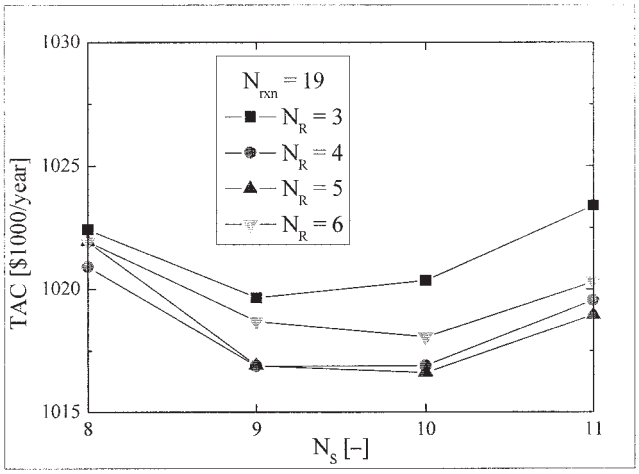

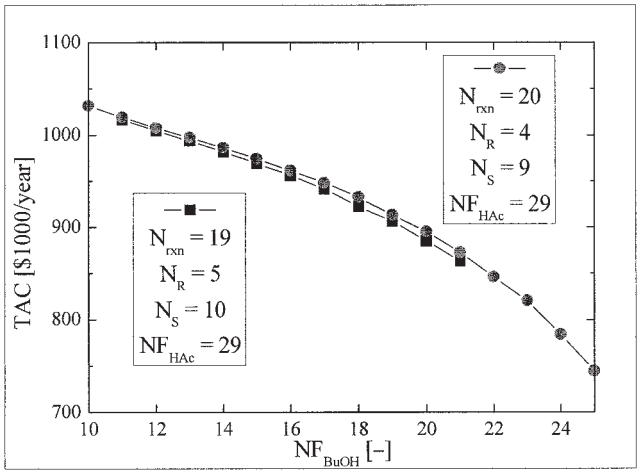

Figure 8. Effects of design variables on TAC for the BuAc system.

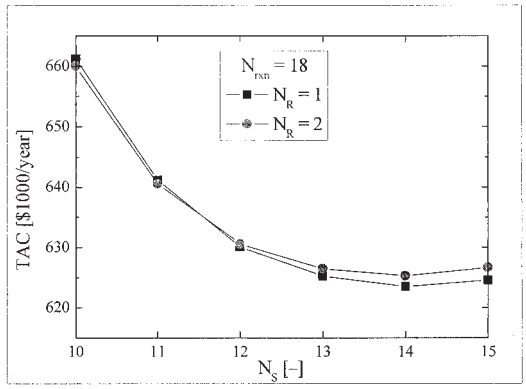

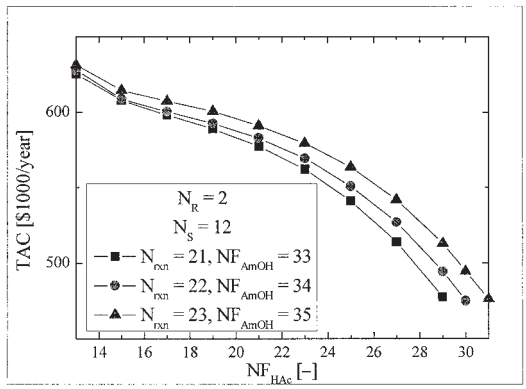

Figure 9. Effects of design variables on TAC for the AmAc system.

Process Characteristics

Type I - MeAc

It is important to recall that the temperature ranking of the MeAc in Table 4 that, for pure components, the order of the normal boiling point temperature is: HAc (118°C) > H_2O(100°C) > MeOH (64.5°C) > MeAc (57.5°C). The composition profile in Figure 10A indicates that we are primarily separating MeOH/H_2O in the rectifying section. This clearly shows the advantage of the reactive distillation by reacting away the heaviest acid toward the bottom part of the reactive zone and consuming the lighter alcohol toward the upper part of the reactive zone. This makes the separation easy by, in a sense, designing the composition for the stripper and the rectifier. The scenario is quite similar to the interaction between reaction section and separation section in the design of recycle plant.[30]

Figure 10A also shows the fraction of total conversion in the reactive zone (shaded area in Figure 10). It reveals that 95% of the total conversion occurs in ~10 reactive trays from the total of 34 reactive trays. The rest of reactive trays (especially toward the upper section of the reactive zone) seem to serve more for the separation purpose by consuming most of the MeOH to facilitate the separation in an almost MeOH free environment. The temperature profile in the MeAc reactive distillation column shows a nonmonotonic temperature distribution (Figure 10B). The reasons come from *reaction* oriented thinking (as opposed to the *separation* oriented thinking) in the

Table 5. Steady-State Operating Condition and Total Annual Cost (TAC) for Reactive Distillation Designs of Five Esterification Systems

System	(i) MeAc	(ii) EtAc		(iii) IPAc		(iv) BuAc	(v) AmAc
Column Configuration	RD	RD	Stripper	RD	Stripper	RD	RD
Total no. of trays including the reboiler	39	20	10	26	8	34	37
No. of trays in stripping section (N_S)	3		9		7	9	12
No. of trays in reactive section (N_{rxn})	34	11		13		20	22
No. of trays in rectifying section (N_R)	1	9		13		4	2
Reactive trays	4∼37	0∼10		0∼12		10∼29	13∼34
Acetic acid feed tray	36	0		0		25	30
Alcohol feed tray	13	0		0		29	34
Feed flow rate of acid (kmol/h)	50.00	48.40		48.20		50.00	50.00
Feed flow rate of alcohol (kmol/h)	50.00	50.00		50.00		50.00	50.00
Top product flow rate (kmol/hr)	50.35	50.30		49.94		50.38	49.98
Bottom product flow rate (kmol/hr)	49.65		48.10		48.26	49.62	50.02
X_D or $X_{D,aq}$							
Acid (m.f.)	0.00087	0.00001		2.5E-6		0.01670	0.00221
Alcohol (m.f.)	0.00556	0.02337		0.02665		0.00688	0.00643
Acetate (m.f.)	0.98000	0.01533		0.00835		0.00076	0.00019
Water (m.f.)	0.01357	0.96129		0.96500		0.97566	0.99117
X_B							
Acid (m.f.)	0.01237		0.00010		0.00002	0.00004	0.00711
Alcohol (m.f.)	0.00763		0.00912		0.00993	0.01006	0.00289
Acetate (m.f.)	$<10^{-8}$		0.99000		0.99000	0.98990	0.99000
Water (m.f.)	0.98000		0.00078		0.00005	$<10^{-8}$	$<10^{-8}$
Condenser duty (kW)	−1280.22	−4265.71	−1860.54	−3428.58	−1129.89	−2857.92	−1483.15
Subcooling duty (kW)		−833.82		−506.51		−461.35	−227.42
Reboiler duty (kW)	1035.71	4523.98	2195.68	3473.31	1370.90	3085.41	1532.48
Column diameter (m)	1.03	1.95	1.45	1.89	1.23	1.88	1.34
Weir height (m)	0.1016	0.1016	0.0508	0.1016	0.0508	0.0508	0.0508
Decanter temperature (°C)		40		50		50	50
Condenser heat transfer area (m^2)	80.03	157.62	68.99	107.37	36.78	57.06	27.63
Subcooling heat transfer area (m^2)		170.24		96.06		57.89	21.82
Reboiler heat transfer area (m^2)	38.63	168.72	92.80	129.53	57.94	115.07	57.15
Damköhler number (Da)	28.88	29.61		13.08		16.86	4.35
Total capital cost ($1000)	730.78	2051.44		1731.74		1277.26	854.62
Column	323.30	511.57		539.56		547.92	408.93
Column trays	50.60	88.10		97.02		111.55	71.85
Heat exchangers	356.88	1451.77		1095.16		617.79	373.84
Total operating cost ($1000/year)	130.55	621.00		474.31		327.53	197.66
Catalyst cost	30.94	64.97		67.06		29.80	16.61
Energy cost	91.55	548.11		399.29		289.26	173.49
Wastewater treatment cost	8.061	7.925		7.965		8.470	7.562
TAC ($1000/year) (50 kmol/hr)	374.14	1304.8		1051.56		753.28	482.54
TAC ($1000/year) (52825 ton/year)	659.14	2005.82		1388.46		850.20	482.54

feed arrangement and, thus, deliberately driving the heavy reactant toward the top and light reactant to the bottom as shown in Figure 10.

The 3-D composition profile in Figure 11 reveals a potential problem for the operation of the MeAc column that the top product MeAc is a saddle and a further increase in the MeAc/H_2O azeotrope in the MeOH free composition space. Figure 12 shows the nonmonotonic behavior in the acetate composition as we change the reflux flow rate while keeping the bottoms water purity at 98%. It should be understandable that control a point near a saddle is not an easy task and reports on the difficulty can be found in the literature (Al-Arafaj and Luyben, 2002).[7]

Type II - EtAc & IPAc

The type II flowsheet differs from the type I in that the two columns (RD column and the stripper) are separated by a decanter. Thus, this flowsheet should be less interacting from steady-state as well as dynamic points of view. The composition profile in Figure 13 indicates that the reactive section generates necessary acetates followed by a rectifying section in which the composition of the heavy acid (HAc) is kept to a ppm level. The overhead vapor is condensed and the condensate falls within the LL envelope, which is further separated by the decanter and high purity H_2O is removed from the aqueous as shown in Figure 11. Part of the organic phase is refluxed back to the RD column while the other part is fed to the stripper to purify EtAc in the left corner of the composition space (Figures 11 and 13), while the top of the stripper is recycled back to the decanter. A straightforward separation is performed in the stripper as shown in the composition profile (Figure 13), and very high purity EtAc can be obtained and the purity level of the acid is the product stream depends on the amount of acid allowed in the overhead of the RD column.

Figure 13 also reveals the 80% of the conversion occurs in the column base of the RD column as a result of large catalyst holdup, high reactant composition, and favorable reaction temperature. The temperature profile in the RD

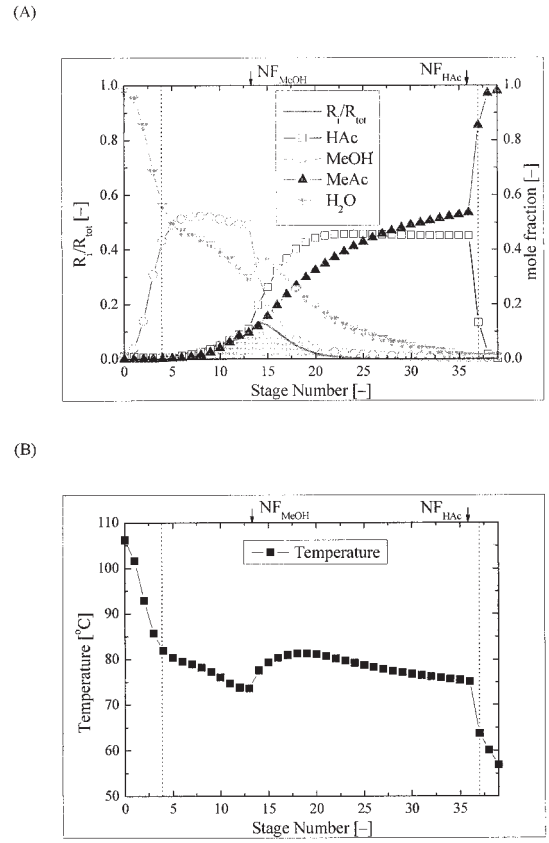

Figure 10. Composition and temperature profiles for the MeAc system.

column shows a monotonic behavior which was dominated by the acid profile.

Very similar composition profile is observed for the IPAc system and, again, most of the conversion takes place in the column base of the RD column (Figure 14). The separation in the stripper is quite straightforward and high purity IPAc can be achieved with little difficulty. The material balance lines in Figure 11 shows how separation is achieved around the decanter.

Type III - BuAc & AmAc

For the BuAc system, the acetic acid has the second highest normal boiling temperature (NBP) and, therefore, the acid is reacting away in the lower part of the reactive zone as shown in Figure 15A. The composition profile in the stripping section clearly shows that the stripper is performing BuOH/BuAc separation. Because of a large LL envelope, only 4 rectifying trays are needed to drive the condensate of the top vapor into the LL zone. It is also observed that significant conversion occurs in the upper section of the reactive zone where two feeds are located nearby. The concentration effects of these two reactants enhance the reaction in that region (Figure 15A). Figure 15B shows an almost monotonic temperature for the reason that these two reactants are close-boiling components with 1°C temperature difference in the NBP's. The vapor and liquid composition profile in a 3-D plot (Figure 11) clearly shows the separation characteristic in the stripping section (along the BuOH/BuAc edge), as well as in the LL envelope.

For the AmAc system, the AmOH has the second highest NBP temperature (which is different from the ranking for the BuAc system). In theory, we should consume most of the alcohol in the reactive zone. Because we do not have stringent product specification on the alcohol, a small amount of AmOH is allowed to leave the reactive zone. Still, the stripping section is performing separation between HAc/AmAc as shown in Figure 16A. Because the AmAc has a larger LL envelope as compared to the BuAc system, only two rectifying trays are required to drive the overhead condensate into the LL zone. Again, majority portion of the reaction takes place in the upper section of the reactive zone where the two feeds are located. However, less reactive trays are required to react away the heavy reactant (as compared to the BuAc system). A nonmonotonic temperature profile is observed as a result of large boiling point temperature difference (~20°C) between these two reactants. Figure 11 shows a different characteristic in the stripping section where the composition distributed along the HAc/AmAc edge.

Results and Discussion

The analyses of the esterification of the acetic acid with five alcohols ranging from MeOH to AmOH (C_1~C_5) are intended to gain insight for the design of reactive distillation by varying the chemical species discretely. As the carbon number in the alcohol increases, the flowsheet changes from type I, to type II, and then to type III (Figure 2). The determinant factors in the flowsheet selection are the ranking of the pure component/azeotrope temperatures (Table 4) and the size of the LL envelope (Figure 1).

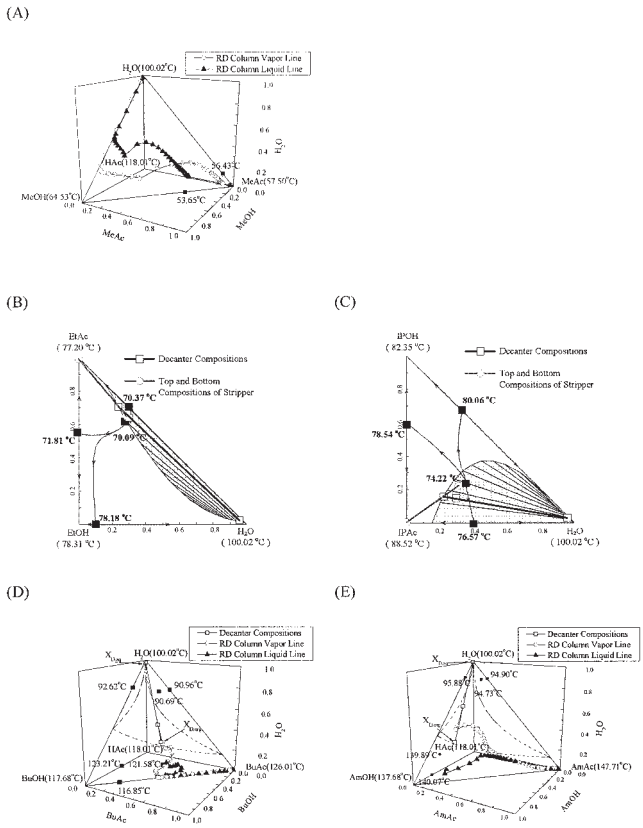

Figure 11. Composition profiles and material balance lines for these five esterification systems.

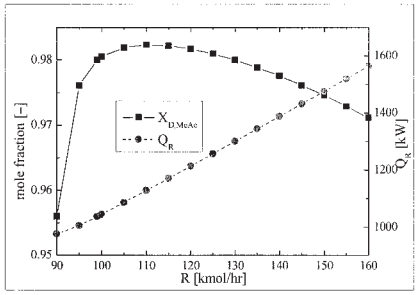

Figure 12. The nonmonotonic behavior in the acetate composition.

That implies the structure of the flowsheet can be determined once the VLLE data become available. The flowsheets may look different in the arrangement; they all include the following units: a stripping section, a reactive zone, and a rectifying section. Once the flowsheet structure is determined, the design can be carried out in a sequential manner by minimizing the TAC. It is interesting to note that most of the dominant design variables are mostly associated with the feed: the feed tray locations (for type I & III) and the feed ratio (for type II). This can be understood because the reactants composition distribution is important for the kinetically controlled reactive distillation. It is also observed that the function of the reactive zone goes beyond providing necessary conversion. The reactive section also facilitates the separation by reacting away the heavy reactant toward the lower part of the reactive zone and by consuming most of the light reactant toward the upper part.

The TAC comparison in Figure 17 shows that the type II (EtAc & IPAc) flowsheet is the most expensive process; followed by type III flowsheet (BuAc & AmAc) and the type I flowsheet is the most economical process. The explanations for this are that the type II flowsheet boils up both products to the top of the RD column (Figure 2) and recycles an almost ternary azeotropic composition back to the decanter from the stripper. Thus, this flowsheet is energy intensive with significant heat-transfer areas. The difference in the TAC's between EtAc and IPAc comes from VLLE advantage of the IPAc system which has a large LL envelope (Figure 1). The type III flowsheet, despite not boiling up both products to the top, needs to boil up some acetate/alcohol along with H_2O upward to get into the LL envelope and then recycles the organic phase *totally* back into the column. One would expect larger energy consumption for this type of system (as compared to systems without a decanter). Again, the difference between BuAc and AmAc lies on the fact that the AmAc system has a larger LL envelope (Figure 1). Finally, the MeAc system (type I) only boils up components necessary to achieve desired product purity and, therefore,

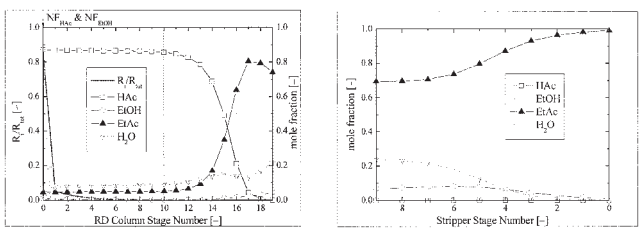

Figure 13. Composition profile and fraction of reaction for the EtAc system.

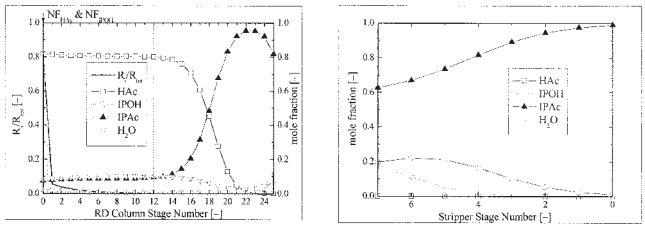

Figure 14. Composition profile and fraction of reaction for the IPAc system.

much smaller energy consumption is expected. Another reason for the MeAc to have the lowest TAC is that the purity level of the acetate is 0.98 (mole fraction) which is typically seen in the literature as compared to 0.99 the other four cases. The reason for the difference is that higher purity levels at both ends (for example, $X_{D,MeAc} = X_{B,H2O} = 0.99$) are not feasible for the MeAc case. However, the purity level difference will not lead to such significant reduction in the TAC.

Conclusion

In this work, the acetic acid esterifications with five different alcohols, ranking from methanol to amyl alcohol (C_1 to C_5),

(A)

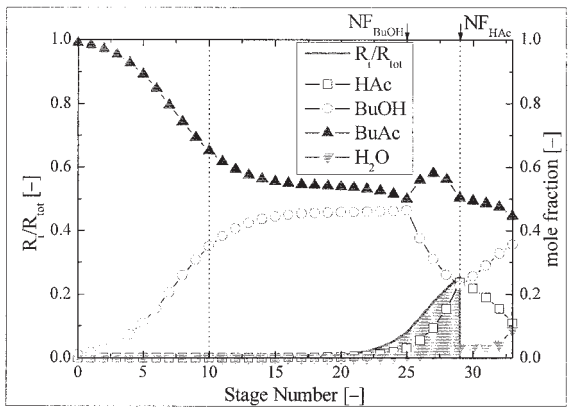

(B)

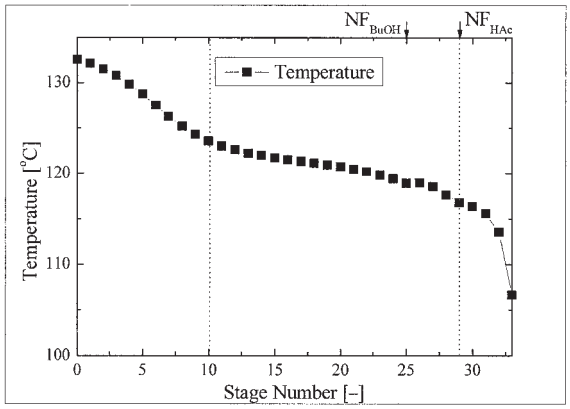

Figure 15. Composition and temperature profiles for the BuAc system.

using the reactive distillation are explored. First, the *qualitative* relationship between phase equilibria and possible process flowsheets is established. Three process flowsheets, type I, II & III, are identified and they all lead to relatively pure products. Two important factors in the flowsheet determination are: (1) the ranking of the pure component/azeotrope boiling point temperature, and (2) the size and the location of the liquid-liquid phase zone. Next, a systematic design procedure is devised to optimize the *quantitative* design based on the total annual cost (TAC). This sequential design procedure overcomes the fragility of the simulation algorithm even with the state-of-the-art process simulator for the reactive distillation. The dominant design variables are also identified and they are: feed locations for the type I flowsheet, feed ratio and the number of trays in the rectifying section for the type II flowsheet, and feed locations for the type III flowsheet. Then, the characteristics of the optimally designed reactive distillation for these three types of flowsheets are investigated explanations are given. Finally, the TAC's of different flowsheets are compared, the economic potential is ranked, and the explanation is given. The results presented in this provide insight for the conceptual design of reactive distillation systems.

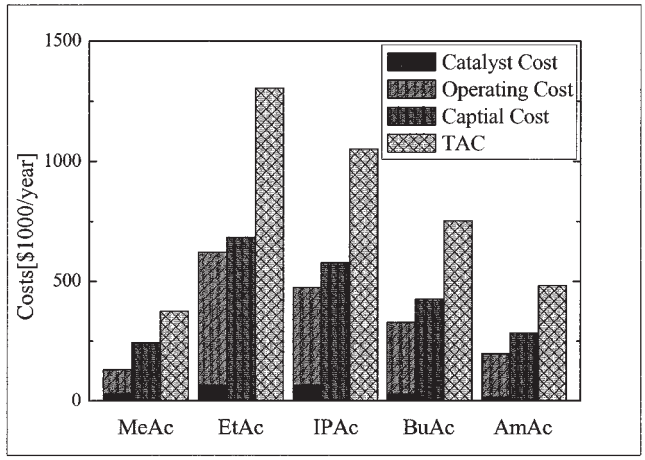

Figure 17. TAC'S (based on 50 kmo1/h production rate) for five esterification systems.

(A)

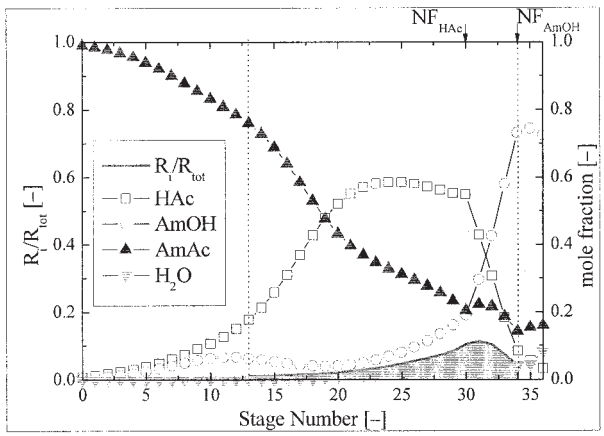

(B)

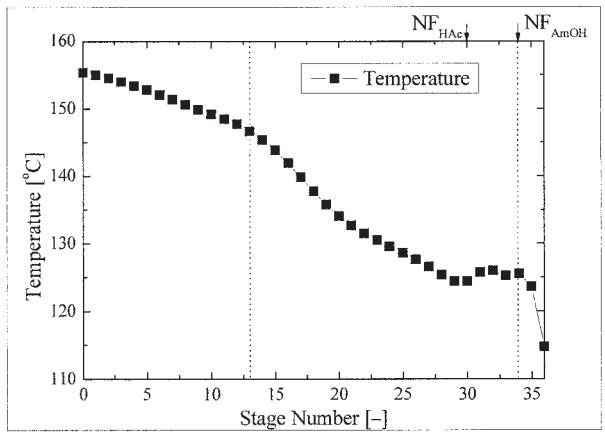

Figure 16. Composition and temperature profiles for the AmAc system.

Acknowledgment

This work is supported by the Ministry of Economic Affairs under grant 92-EC-17-A-09-S1-019. We also thank Y. L. Liu and China Petrochemical Development Corp. for providing wastewater treatment costs for TAC calculation.

Notation

$AmAc$ = Amyl acetate
$AmOH$ = Amyl alcohol (n-pentanol)
$BuAc$ = n-butyl acetate
$BuOH$ = n-butanol
Da = Damköhler number for the whole column
$EtAc$ = ethyl acetate
$EtOH$ = ethanol
F_{Acid} = acid feed flow rate
$F_{Alcohol}$ = alcohol feed flow rate
FR = feed ratio
$IPAc$ = isopropyl acetate
$IPOH$ = isopropanol
$MeAc$ = methyl acetate
$MeOH$ = methanol
NF_{Acid} = acid feed location
$NF_{Alcohol}$ = alcohol feed location
NF_{heavy} = heavy reactant feed location
NF_{light} = light reactant feed location
N_R = number of trays in the rectifying section
N_{rxn} = number of trays in the reactive section
N_S = number of trays in the stripping section
N_T = total number of trays
Q_C = condenser duty
Q_R = reboiler duty of the reactive distillation column
$Q_{R,S}$ = reboiler duty of the stripper
R = reflux flow rate
r = reaction rate
R_i = reaction on tray i
R_{tot} = total reaction in the column
k_1 = forward rate constant
k_{-1} = backward rate constant
K_{eq} = equilibrium constant for the esterification reaction
m_{cat} = catalyst-weight
TAC = total annual cost
X_B = liquid mole fraction in the bottom product
X_D = liquid mole fraction in the distillate
$X_{D,org}$ = organic liquid mole fraction in the decanter

$X_{D,\,aq}$ = aqueous liquid mole fraction in the decanter

Literature Cited

1. Doherty MF, Malone MF. *Conceptual Design of Distillation System*, New York: McGraw-Hill; 2001.
2. Sundmacher K, Kienle A. *Reactive Distillation: Status and Future Directions*, Wiley-VCH Verlag GmbH & Co. KGaA, Weinheim: Germany; 2003.
3. Taylor R, Krishna R. Modelling Reactive Distillation. *Chem Eng Sci.* 55:5183; 2000.
4. Doherty MF, Buzad G. Reactive Distillation by Design. *Trans IchemE.* A70:448;1992.
5. Agreda VH, Partin LR, Heise WH. High Purity Methyl Acetate via Reactive Distillation. *Chem Eng Prog*. 86(2):40;1990.
6. Kaymak DB, Luyben WL. Quantitative comparison of reactive distillation with conventional multiunit reactor/column/recycle systems for different chemical equilibrium constants. *Ind Eng Chem Res.* 43:2493; 2004.
7. Al-Arafaj MA, Luyben WL. Comparative control study of ideal and methyl acetate reactive distillation. *Chem Eng Sci.* 57:5039;2002.
8. Burkett RJ. Rossiter D. Choosing the right control structure for industrial distillation columns. *Proc. of Process Control and Instrumentation 2000*: Glasgow; UK 38;2000.
9. Kenig EY, Bader H, Gorak A, Bebling B, Adrian T, Schoenmakers T. Investigation of ethyl acetate reactive distillation process. *Chem Eng Sci.* 56:6185;2001.
10. Hanika J, Smejkal Q,. Kolena J. Butylacetate vis reactive distillation-modelling and experiment. *Chem Eng Sci.* 54:5205;1999.
11. Gangadwala J, Kienle A, Stein E,. Mahajani S. Production of butyl acetate by catalytic distillation: Process design studies. *Ind Eng Chem Res.* 43:136;2004.
12. Steinigeweg S,. Gmehling J. *n*-Butyl acetate synthesis via reactive distillation: thermodynamic aspects, reaction kinetics, pilot-plant experiments, and simulation studies. *Ind. Eng. Chem. Res.* 41:5483;2002.
13. Pöpken T, Götze L, Gmehling J. Reaction kinetics and chemical equilibrium of homogeneously and heterogeneously catalyzed acetic acid esterification with methanol and methyl acetate hydrolysis. *Ind Eng Chem Res.* 39:2601;2000.
14. Hangx G, Kwant G, Maessen H, Markusse P, Urseanu I. *Reaction Kinetics of the Esterification of Ethanol and Acetic Acid Towards Ethyl Acetate. Deliverable 22, Intelligent Column Internals for Reactive Separations (INTINT)*. Technical Report to the European Commission; 2001. http://www.cpi.umist.ac.uk/intint/NonConf_Doc.asp.
15. Gadewar SB, Malone MF,. Doherty MF. Feasible region for a countercurrent cascade of vapor-liquid CSTRs. *AIChE J*. 48:800;2002.
16. Gangadwala J, Mankar S, Mahajani S, Kienle A, Stein E. Esterification of acetic acid with butanol in the presence of ion-exchange resins as catalysts. *Ind Eng Chem Res.* 42:2146;2003.
17. Lee MJ,. Wu HT, Kang CH, Lin HM. Kinetic behavior of amyl acetate synthesis catalyzed by acidic cation exchange resin. *J Chin Inst Chem Eng.* 30:117;1999.
18. Renon H, Prausnitz JM. Local compositions in thermodynamics excess functions for liquid mixtures. *AIChE J.* 14:135;1968.
19. Hayden JG, O'Connell JP. A generalized method for predicting second virial coefficients. *Ind Eng. Chem. Process Des. Dev.* 14:209;1975.
20. Huang SG, Yu CC. Sensitivity of thermodynamic parameter to the design of heterogeneous reactive distillation: Amyl acetate esterification. *J Chin Inst Chem Eng.* 34:345;2003.
21. Chiang SF, Kuo CL, Yu CC, Wong DSH. Design alternatives for the amyl acetate process: Coupled reactor/column and reactive distillation. *Ind Eng Chem Res.* 41:3233;2002.
22. Horsley LH. *Azeotropic Data – III*. Washington, D.C; Advances in Chemistry Series No. 116;1973. American Chemical Society.
23. Komatsu H, Holland CD. A new method of convergence for solving reacting distillation problems. *J Chem Eng Japan*. 10:292;1977.
24. Vora N, Daoutidis P. Dynamic and control of an ethyl acetate reactive distillation column. *Ind Eng Chem Res.* 40:833;2001.
25. Lee JW. Feasibility studies on quaternary reactive distillation systems. *Ind Eng Chem Res.* 41:4632;2002.
26. Tang YT, Huang HP, Chien I-L. Design of a complete ethyl acetate reactive distillation system. *J Chem Eng Japan*. 36:1352;2003.
27. Lee LS, Kuo MZ. Phase and reaction equilibria of the acetic acid-isopropanol-isopropyl acetate-Water system at 760 mmHg. *Fluid Phase Equilib.* 12:147;1996.
28. Huang SG, Kuo CL,. Hung SB, Chen YW, Yu CC. Temperature control of heterogeneous reactive distillation: Butyl propionate and butyl acetate esterification. *AIChE J.* 51(9): 2203; 2004.
29. Douglas, JM. *Conceptual Design of Chemical Process*, New York: McGraw-Hill; 1988.
30. Cheng YC. Yu CC. Effects of process design on recycle dynamics and its implication to control structure selection. *Ind Eng Chem Res.* 42:4348;2003.
31. Elliott TR, Luyben WL. Quantitative assessment of controllability during the design of a ternary system with two recycle streams. *Ind Eng Chem Res.* 35:3470;1996.
32. Venimadhavan G, Malone MF. Doherty MF. A novel distillate policy for batch reactive distillation with application to the production of butyl acetate. *Ind Eng Chem Res.* 38:714;1999.

Appendix A.

TAC calculation

The equipment cost estimation follows the procedure of Douglas[29] and specific equations of Elliott and Luyben,[31] and Chiang et al.[21] were used. A payback period of 3 years is assumed, and a M&S index of 1108.1 is used in the calculation. Materials of construction are stainless steel. The equipment is sized as follows:

(1) Reboiler heat-transfer area (A_R)

$$A_R[\mathrm{m}^2] = \frac{Q_R}{U_R \cdot \Delta T_R} \tag{A1}$$

where Q_R [W] is the reboiler duty, the overall heat-transfer coefficient U_R is assumed 788.45 W/(m^2*K), and the temperature driving forceΔ T_R [K] in the reboiler depends on the steam.

(2) Condenser heat-transfer area (A_C)

$$A_C[\mathrm{m}^2] = \frac{Q_C}{U_C \cdot \Delta T_C} \tag{A2}$$

where Q_C [W] is the condenser duty, the overall heat-transfer coefficient U_C is assumed 473.07 W/(m^2*K), and the log-mean temperature driving force Δ T_C [K] depends on the dew points and bubble points for a total condenser.

(3) Column diameter (D_C)

$$D_C[\mathrm{m}] = \sqrt{\frac{5.67 \times 10^{-8}}{\pi}\left(\frac{M_W^2}{\rho_V}\right)^{1/2}}\, V^{1/2} \tag{A3}$$

where V [kmol/h] is the maximum vapor flow rate, ρ_V [kg/m^3] is the vapor density in the column, and M_W [kg/kmol] is the average molecular weight.

(4) Column height (L_C)

$$L_C[\mathrm{m}] = 0.7315 N_T \tag{A4}$$

where N_T is the total number of trays.

The capital and operating costs are calculated according to:

(1) Column cost

$$\text{Column cost [\$]} = \frac{M\,\&\,S}{280}(101.9D_C^{1.066}L_C^{0.802}(2.18 + F_C)) \quad \text{(A5)}$$

where $F_C = F_mF_p = 3.67 \cdot 1$.

(2) Tray cost

$$\text{Tray cost [\$]} = \frac{M\,\&\,S}{280}(4.7D_C^{1.55}L_CF_C) \quad \text{(A6)}$$

where $F_C = F_s + F_t + F_m = 1 + 1.8 + 1.7$.

(3) Heat exchanger cost

$$\text{Heat exchanger cost [\$]} = \frac{M\,\&\,S}{280}(A^{0.65}(2.29 + F_C)) \quad \text{(A7)}$$

where $F_C = (F_d + F_p)F_m = (1.35 + 0) \cdot 3.75$ for the reboiler and $F_C = (F_d + F_p)F_m = (1 + 0) \cdot 3.75$ for the condenser.

(4) Steam cost

$$\text{Steam cost}\left[\frac{\$}{\text{year}}\right] = \frac{\$C_S}{453.59\ \text{kg}}\left(\frac{Q_R}{\lambda_V}\right)\left(8150\,\frac{\text{h}}{\text{year}}\right) \quad \text{(A8)}$$

where C_s is the saturated steam price and is the latent heat of the steam which depends on the bottom temperature.

(5) Cooling water cost

$$\text{Cooling water cost}\left[\frac{\$}{\text{year}}\right]\text{Cooling water cost}\left[\frac{\$}{\text{year}}\right] = \frac{\$0.03}{3.785\ \text{m}^3}\left(\frac{0.001\ \text{m}^3}{\text{kg}}\right)\left(\frac{Q_C}{30}\right)\left(8150\,\frac{\text{h}}{\text{year}}\right) \quad \text{(A9)}$$

(6) Catalyst cost (assuming a catalyst life of 3 months)

$$\text{Catalyst cost [\$]} = \text{catalyst loading [kg]} \cdot 7.7162\,\frac{\$}{\text{kg}} \quad \text{(A10)}$$

Appendix B.

Wastewater treatment TAC calculation

The wastewater (WW) is treated in a two-stage structure. First, the WW is neutralized and processed in an on-site biological WW treatment facility, followed by a central WW processing unit in the industrial park (denoted as IPCC cost). The following table (Table B1) describes the on-site and IPCC costs, and the total operating cost is computed accordingly.

Manuscript received July 23, 2004, and revision received Oct. 21, 2004.

Table B1. Wastewater Treatment Cost

Item	Unit Price	Consumption	MeAc Cost ($/year)	EtAc Cost ($/year)	IPAc Cost ($/year)	BuAc Cost ($/year)	AmA Cost ($/year)
Mass flow rate (ton/year)			8164.32	8646.12	8689.92	8392.08	8138.04
NaOH Requirement (ton/year)			481.8	0.3854	0.096	648.24	85.848
NaOH	0.0012 ($/kg)		578.160	0.463	0.116	777.888	103.018
Electricity	0.0529 ($/kWhr)	5.6 (kWhr/ton)	2418.598	2561.327	2574.302	2486.070	2410.813
H_3PO_3	0.2941 ($/kg)	0.057 (kg/ton)	136.864	144.941	145.675	140.682	136.424
Sludge incineration	0.0605 ($/kg)	5.350 (kg/ton)	2642.586	2798.533	2812.710	2716.306	2634.080
IPCC-COD	0.4817 ($/kg)	0.2 (kg/ton)	786.551	832.967	837.187	808.493	784.019
IPCC-SS	0.8632 ($/kg)	0.1 (kg/ton)	704.744	746.333	750.114	724.404	702.476
IPCC-water	9.73E-5 ($/kg)	1000 (kg/ton)	793.753	840.594	844.853	815.896	791.198
TAC ($1000/year)			8.061	7.925	7.965	8.470	7.562